Wireless Memory Approximation for Energy-efficient Task-specific IoT Data Retrieval

Junya Shiraishi, Shashi Raj Pandey, Israel Leyva-Mayorga, and Petar Popovski Department of Electronic Systems, Aalborg University.

Email: {jush, srp, ilm, petarp}@es.aau.dk.

Abstract—The use of Dynamic Random Access Memory (DRAM) for storing Machine Learning (ML) models plays a critical role in accelerating ML inference tasks in the next generation of communication systems. However, periodic refreshment of DRAM results in wasteful energy consumption during standby periods, which is significant for resource-constrained Internet of Things (IoT) devices. To solve this problem, this work advocates two novel approaches: 1) wireless memory activation and 2) wireless memory approximation. These enable the wireless devices to efficiently manage the available memory by considering the timing aspects and relevance of ML model usage; hence, reducing the overall energy consumption. Numerical results show that our proposed scheme can realize smaller energy consumption than the always-on approach while satisfying the retrieval accuracy constraint.

Index Terms—dynamic random access memory, energy efficiency, goal-oriented communication, memory approximation.

I. Introduction

THE use of lightweight, on-device Artificial Intelligence (AI)/Machine Learning (ML) models can empower Internet of Things (IoT) devices to transmit only data that is critical for the specific downstream tasks [1]. This allows each IoT device to reduce its energy consumption. For example, introducing TinyML can significantly reduce energy waste of IoT devices by letting them filter out irrelevant data transmissions [2]. Related work on goal-oriented communications, such as task-specific IoT data retrieval and semantic queries [2], largely focuses on designing energy-efficient communication protocols by running AI/ML algorithms on devices for the semantic extraction and interpretation of data locally. While memory management is not commonly considered a factor for energy consumption, it can have a major impact on IoT devices. This is especially true in the context of intelligent 6G networks, where the IoT devices have intelligent modules, such as TinyML, and their transmissions are conditioned on the inferences carried out by these modules [2].

Dynamic Random Access Memory (DRAM) technology is used in a wide range of systems, including, intelligent IoT camera systems for real-time operation. During the operation of such systems, the energy consumption of DRAM can be divided into two parts: 1) data storage and access, and

The work of J. Shiraishi was supported by European Union's Horizon Europe research and innovation funding programme under Marie Skłodowska-Curie Action (MSCA) Postdoctoral Fellowship, "NEUTRINAI" with grant agreement No. 101151067. The work of P. Popovski was supported by the Velux Foundation, Denmark, through the Villum Investigator Grant WATER, nr. 37793.

2) memory refreshment. Specifically, throughout a standby period, DRAM needs a periodic refreshment due to its volatility. This refreshment dominates the energy consumption of the device [3], [4], which consumes up to 50% of total energy consumption of DRAM [5]. Importantly, the device should keep refreshing its memory even if in the absence of a computation requirement. This is necessary to be able to swiftly respond to the arrival of a computational task quickly. The energy waste due to standby-mode memory refreshments has received relatively low attention in the research literature, as compared to the energy reduction technology during the idle-period of communication [6].

Memory approximation is an attractive approach to reduce energy consumption [5], [7], in which the DRAM refresh rate is reduces, lowering the energy consumed by the refreshment at the cost of deterioration of accuracy. In [3], the memory controller adapts the refreshing time considering data importance or criticality. In [8], content-aware refresh has been proposed aiming to reduce the total number of times that the memory is refreshed. The concept of approximation of DRAM memory is investigated for smart camera systems, considering the cost of communication, sensing, processing, and memory access [9]. However, it does not consider how to reduce the wasteful memory access during the stand-by period, considering the timing and relevance to the current tasks of the receivers. Using memory irrespective of its importance for the current task is clearly a waste of energy. In order to solve the above-mentioned problem, this paper brings two concepts inspired by goal-oriented communication [10]: i) wireless memory activation and ii) wireless memory approximation (c.f. Sec. II-A). The fundamental principles of both concepts are to use memory only at right timing and only for the relevant model, as summarized follow:

- Wireless memory activation: Realizing remote activation of memory of IoT device at the specific timing.
- Wireless memory approximation: Remotely approximating memory use by specifying the refresh period of DRAM memory considering the importance level of specific ML model to serve the requested tasks.

These concepts enable the IoT device to spend energy at the memory only when the specific model is highly likely required to complete the future task, leading to the significant energy reduction for memory use during the stand-by period.

To formalize and validate the concepts of wireless memory activation and approximation, this work focuses on a particular low-latency remote inference scenario, where the Edge Server (ES) is interested in retrieving task-specific data with low latency to serve the user's requirement. The specific applications include wireless image retrieval tasks in IoT networks as in [2]. Our contributions can be summarized as follows: *i*) We propose wireless memory activation and approximation for energy-efficient task-specific IoT data retrieval; *ii*) We introduce a pull-based communication framework and design an associated energy-efficient communication/memory access protocol that takes into account the timing of memory use for the relevant ML model; *iii*) We characterize the system-level performance of the proposed scheme and elicit the gain in terms of total energy consumption and retrieval accuracy.

II. SYSTEM MODEL

We consider a simplified setup to elucidate the memory activation/approximation problem. The network consists of an ES, a single IoT device equipped with vision sensor, a radio interface, memory controller, DRAM, and a storage, and an external service requester (user). Each of these entities communicates over a wireless medium. We consider a pull-based communication system in which the ES is conducting a specific task of data collection from the IoT device, as requested by the external user.

The external user requests the data acquisition task to the ES, which follows a Poisson process with the average arrival rate λ [query/s]. We define the time of the previous query arrival as 0 and use t_q to denote the random variable that represents the current query instance (episode). To facilitate our analysis of the gain brought by our method (c.f. Sec. II-A), this work focuses on the behavior of memory on the specific instance of the task-specific IoT data retrieval, i.e., the memory behavior of IoT device during the duration of $[0,t_q]$.

Upon receiving this query request from the external user, the ES forwards a query to the target IoT device. The IoT device detecting this query, processes and transmits the data, such as the estimated label obtained by ML model, to the ES. We further assume an error-free channel for both uplink and downlink communication.

Furthermore, we assume that the ES has perfect knowledge about λ based on the data collected in the past, but the actual query timing is unknown. The goal of this work is to design an energy-efficient data transmission framework that facilitates timely acquisition of only the relevant data, defined through user query, while considering the overall cost of memory usage. This involves wireless remote memory activation and approximation procedure, as illustrated in the system overview in Fig. 1, and discussed next.

A. Wireless Memory Activation and Approximation

Now, we introduce the concept of wireless memory activation and approximation. The basic idea is illustrated in Fig. 1. When a new episode begins at t=0, the ES first decides the timing of the transmission of the memory activation signal based on the statistical knowledge that the ES has about the query arrival for the specific task, i.e., average arrival rate λ . Specifically, the ES transmits a memory activation

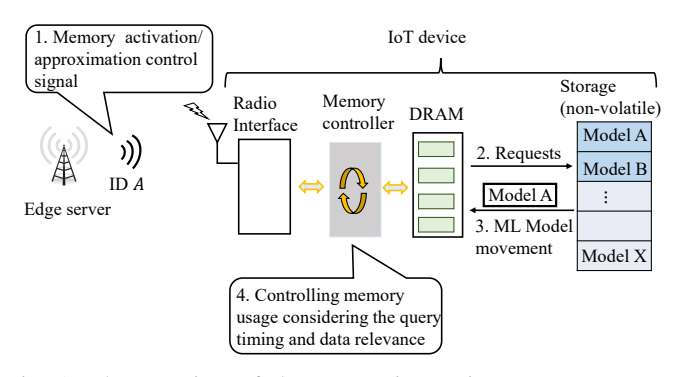


Fig. 1: The overview of the system integrating remote memory activation/approximation.

signal at ζ [s] after the current episode begins. The memory activation signal includes the information of the specific model to be moved to the memory related to the current task, e.g, by embedding the model Identity (ID) information into the control signal (e.g. model ID A). If the receiver of IoT device detects this control signal, it checks whether it satisfies the model activation conditions. Specifically, it checks whether information of model ID embedded into control signal coincides with the model ID stored in the storage. If so, it moves the specific model \mathcal{M}_A from the storage to the memory. Then, each device initiates processing using the ML model. This enables demand-driven DRAM activation, reducing wasteful energy consumption during the stand-by periods. After sending the memory activation signal, the ES sends the memory approximation signal so that it can set the refresh period to be τ . Longer τ means that ES can accept higher information loss, that is, coarser data approximation. The wireless memory approximation aims to remotely control the refresh period of memory based on the importance of each model in terms of expected future demand from the external user. For example, when the ES knows the data point X (such as feature map) is more important than the data point Y, it is reasonable to allocate a small (large) refresh period for data point X(Y) to efficiently control the efficient memory use. To this end, one could send a control signal or a behavior model so that the IoT device can autonomously tune the memory approximation based on the installed model. This work focuses on the former approach.

The total overhead required for the wireless memory activation and approximation is $T_{\Sigma} = T_W + T_{\rm approx} + T_l$, where T_W , $T_{\rm approx}$, and T_l , respectively, represent the time required for control signal transmission, the additional overhead required for notifying the approximation of the model, and the time required for loading the model.

B. DRAM Retention Accuracy

DRAM must be continuously refreshed to retain the data, as the content is volatile due to capacitor discharge. The refresh interval τ is a key to control the quality of data in the memory, i.e., to control the level of approximation of DRAM. A larger refresh interval τ can reduce the energy use of memory, while it increases the chances of bit errors in DRAM [11], as capacitors may discharge below a threshold needed to

retain information [9]. Normally, DRAM is responsible to store the images and different Deep Neural Networks (DNN) parameters, including weights and feature maps [9]. The focus of this work is to characterize the accuracy of ML model through the different refresh rate and the timing of memory activation. To enable the adaptation of different refresh interval, it needs to introduce different quality bins $\mathcal{Q} = \{q_1, q_2, \ldots, q_{I_{\mathrm{M}}}\}$, each of which is allocated a different refresh period. Here, a larger quality bins represents a higher refresh interval, leading to a higher bit error. Then, each data point, e.g., ML model for the specific task will be assigned to one of the quality bin in \mathcal{Q} , based on the mapping function.

To characterize the accuracy degradation through the parameter of τ and ζ , we model the state of each memory array with two state Markov chain, consisting of correct state and erroneous state. Here, each memory array is assumed to be in the correct state when it is loaded. In each refreshment, the state transition from the correct state to error state happens with probability $P_e(\tau)$, depending on the refresh period τ :

$$P_e(\tau) = 1 - \exp\left(-\frac{\tau - \tau_0}{\beta}\right),\tag{1}$$

where $\tau_0=64$ [ms] is the refresh time required to maintain the data in DRAM without error and β is a hardware specific constant value representing the degree of accuracy degradation; smaller (larger) β corresponds to the case where the speed of memory degradation is higher (lower). On the other hand, we model that the error state is an absorbing state, meaning that after entering an erroneous state, it no longer returns to the correct state. Given the refresh period τ and total memory activation period $Q=t_q-\zeta$, the total number of refreshments during a single episode is $M_\zeta=\lfloor\frac{Q}{\tau}\rfloor$. Then, the probability that the state is in the erroneous state after M_ζ refreshments can be expressed as:

$$\bar{P}_e(M_\zeta, \tau) = 1 - (1 - P_e(\tau))^{M_\zeta}$$
 (2)

In this work, to facilitate our analysis, we assign a unique refresh period τ for all data points $\boldsymbol{x} = [x_1, x_2, \dots, x_N]^\top$ to analyze the system-level trade-off between accuracy and energy, where N is the total number of bits stored in the DRAM. In practice, the refresh period τ should be decided given data point \boldsymbol{x} considering the maximum allowable distortion $\Delta \in [0,1]$. To define allowable distortion Δ , this paper considers Hamming distortion. Let $\boldsymbol{y} = [y_1, y_2, \dots, y_N]^\top$ be the decayed data point of \boldsymbol{x} . Then, the Hamming distortion between \boldsymbol{x} and \boldsymbol{y} is expressed as:

$$d(\boldsymbol{x}, \boldsymbol{y}) = \frac{1}{N} \sum_{j=1}^{N} \mathbb{1}(x_j \neq y_j).$$
 (3)

Finally, we define retention accuracy, the accuracy threshold that the ML model can retain in memory, as $d(\boldsymbol{x}, \boldsymbol{y}) \leq \Delta$, based on the predefined threshold Δ . Accordingly, we can derive retention accuracy, which is the probability that the model can provide correct output after M_{ζ} refreshments based on Hamming distortion. Formally, given Δ and Q, the

retention accuracy, defined as $\gamma(\tau,Q) = \Pr(d(x,y) \leq \Delta)$ can be expressed as:

$$\gamma(\tau, Q) = \sum_{k=0}^{\lfloor N\Delta \rfloor} {N \choose k} \bar{P}_e \left(M_{\zeta}, \tau \right)^k \left(1 - \bar{P}_e(M_{\zeta}, \tau) \right)^{N-k}. \tag{4}$$

C. Retrieval Accuracy

The retrieval accuracy, i.e., the accuracy of received data with respect to the specific task can be defined by considering two aspects: 1) whether the ES successfully collects data from the IoT device and 2) the accuracy of output of ML model in Eq. (4). Formally, we define the retrieval accuracy as follows:

$$U(\tau, \zeta, T_{\Sigma}) = h(\zeta)\gamma(\tau, Q), \tag{5}$$

where $h(\zeta) \in \{0,1\}$ is a Bernoulli random variable, representing whether the ES successfully received task-specific data from the IoT device upon the query request. Under the error-free channel, the ES can successfully receive the data related to the current task only if the memory is activated by the time t_q . Here, $h(\zeta)=1$ only if it satisfies $(\zeta+T_\Sigma)< t_q$; otherwise $h(\zeta)=0$. On the other hand, the accuracy of ML model $\gamma(\tau,Q)$ depends on the local inference accuracy, influenced by the refresh period τ and Q.

D. Energy Model

The total energy consumption of an IoT device, $E_{\rm tot}(t_q)$ can be calculated by taking into account the energy consumed for i) communication, $E_{\rm c}(t_q)$, ii) computation, $E_{\rm p}(t_q)$, iii) refreshment, $E_{\rm re}(t_q)$, and iv) ML model loading from the storage to memory, $E_{\rm l}(t_q)$, during a single episode.

The energy consumed for refreshment depends on the total number of refreshment during a single episode, denoted as $n_{\rm re}(\tau,\lambda)$, which is a function of λ and the refresh period τ . Then, let $b_{\rm row},I_M$, and $\xi_{\rm re}$ be the data size that can be stored in a single row in DRAM, the total number of bins that the IoT device uses during a single episode, and the energy consumption for the refreshment of DRAM row, respectively. Then, the total energy consumed for refreshment becomes:

$$E_{\rm re}(t_q) = \xi_{\rm re} n_{\rm re}(\tau, \lambda) I_M b_{\rm row}. \tag{6}$$

On the other hand, we model the energy required by the other units as: $E_{\rm c}(t_q)+E_{\rm p}(t_q)=w_cI_{\rm M}\xi_{\rm re}$ and $E_{\rm l}(t_q)=w_lI_{\rm M}\xi_{\rm re}.$ Here, w_c and w_l are, respectively, a scaring factor controlling the ratio of energy consumption of $E_{\rm c}(t_q)+E_{\rm p}(t_q)$ and $E_{\rm l}(t_q)$ against the energy consumed for the single refreshment.

III. ANALYSIS AND PROBLEM FORMULATION

The retrieval accuracy and total energy consumption of the proposed scheme is derived based on the the analytical model illustrated in Fig. 2.

Considering the Probability Density Function (PDF) of query arrival time and the definition of retrieval accuracy

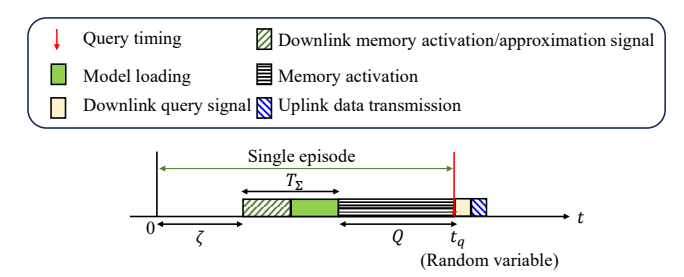


Fig. 2: Analytical model.

defined in Eq. (4), the expected retrieval accuracy of our proposed scheme can be expressed as follows:

$$\mathbb{E}[U^{\mathcal{P}}(\tau,\zeta,T_{\Sigma})] = \sum_{k=0}^{\lfloor N\Delta \rfloor} \Pr(N_{e}(M_{\zeta}) = k)$$

$$= e^{-\lambda (\zeta + T_{\Sigma})} \sum_{k=0}^{\lfloor N\Delta \rfloor} (1 - \psi) \binom{N}{k} \sum_{j=0}^{k} \frac{\binom{k}{j}(-1)^{j}}{1 - \psi q_{e}^{c}}, \tag{7}$$

where $\psi = \exp(-\lambda \tau)$, c = N - k + j, and $q_e = 1 - P_e$.

On the other hand, based on the energy model mentioned in Sec. II-D, the total energy consumption of the proposed scheme during a single episode can be expressed as follows:

$$\mathbb{E}[E_{\text{tot}}^{\text{p}}] = e^{-\lambda (\zeta + T_{\Sigma})} \left(\frac{\psi}{1 - \psi} + w_c + w_l \right) I_{\text{M}} \xi_{\text{re}}. \tag{8}$$

See the Appendix for the detailed derivation of Eqs. (7)– (8). Considering the trade-off between the retrieval accuracy and total energy consumption through the values of $\{\zeta, \tau\}$, here, we evaluate the minimum energy consumption under the retrieval accuracy constraint $U_{\rm th}$, formulated as:

$$\min_{\{\tau,\zeta\}} \mathbb{E}[E_{\text{tot}}^{\text{p}}] \text{ s.t. } \mathbb{E}[U^{\text{p}}] \geq U_{\text{th}}. \tag{9}$$

Here, as the problem in Eq. (9) is non-convex, we rely on the grid-search method to find the optimal solution. Specifically, we select the value of ζ in the range from 0 to 250 with a step of 0.5, and that of τ in the range from 64 ms to 2560 ms with a step of 64 ms.

IV. NUMERICAL EVALUATIONS

In this section, we present results for the retrieval accuracy and the normalized energy consumption for the different parameters. These results were obtained through Monte Carlo simulation, with over 10^4 trials, based on the description of Sec. II and obtain the results of the analysis described in Sec. III.

As a baseline scheme, we consider the always-on approach, in which DRAM remains active holding the task-specific ML model during the entire episode, in which the memory is refreshed with periodicity τ_0 . For the sake of brevity, we omit the detail here, but the retrieval accuracy and total energy consumption of baseline scheme can be expressed as $\mathbb{E}[U^{\rm b}]=1$ and $\mathbb{E}[E^{\rm b}_{\rm tot}]=\left(\frac{\psi_0}{1-\psi_0}+w_c\right)I_{\rm M}\xi_{\rm re}$, where $\psi_0=e^{-\lambda\,\tau_0}$. Here, the normalized energy consumption of

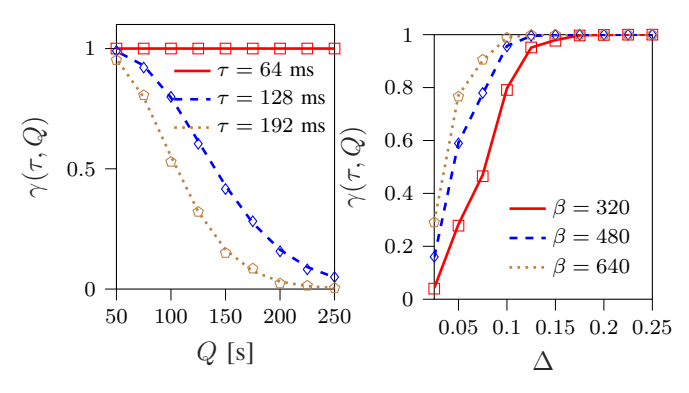


Fig. 3: Retention accuracy defined in Eq. (4) as a function of memory activation period Q (left figure) and Δ (right figure) for the results obtained by Eq. (4) (line) and by simulations (marker).

the proposed scheme can be defined as $\bar{E} = \mathbb{E}[E_{\text{tot}}^{\text{p}}]/\mathbb{E}[E_{\text{tot}}^{\text{b}}]$, which can be expressed as follows:

$$\bar{E} = e^{-\lambda (\zeta + T_{\Sigma})} \frac{(1 - \psi_0)\psi + (w_c + w_l)(1 - \psi_0)(1 - \psi)}{\psi_0(1 - \psi) + (1 - \psi_0)(1 - \psi)w_c}.$$
(10)

A. Numerical Results

1) Behavior of DRAM Retention Accuracy Model: Fig. 3 (left) shows retention accuracy in Eq. (4) as a function of memory activation period Q, where we set N=64, $\beta=$ 640 and $\Delta = 0.1$. From this figure, we can see that the retention accuracy $\gamma(\tau, Q)$ becomes small as refresh period τ becomes large, because of the increase of the probability to transit in the error state in Eq. (1). Next, we can also see the retention accuracy decreases as the memory activation period Q increases. This is because the probability of error after M_Q refreshments $\bar{P}_e(M_\zeta, \tau)$ in Eq. (2) becomes larger. Next, Fig. 3 (right) shows retention accuracy $\gamma(\tau, Q)$ against the retention accuracy threshold Δ , where we set Q = 50 and $\tau =$ 128 ms. From this figure, we can see that retention accuracy increases as Δ becomes larger as it allows more number of erroneous state for an memory array after M_{ζ} refreshments. Next, we can see that retention accuracy $\gamma(\tau, Q)$ increases as β becomes larger. This is because higher β reduces $P_e(\tau)$ in Eq. (1), leading to the reduction of $\bar{P}_e(M_{\zeta}\tau)$ and increases $\gamma(\tau, Q)$.

2) Impact of ζ : Fig. 4 shows the retrieval accuracy and normalized energy consumption, \bar{E} , against the time passed for sending the memory activation signals ζ for the different query arrival rate λ , where we set $\beta=6400$, $\tau=128$ ms, N=64, $\Delta=0.1$, $T_{\Sigma}=0$, $w_{\rm c}=0$, and $w_{\rm l}=0$. From this figure, we can first see that the results of \bar{E} and retrieval accuracy obtained by our theoretical analysis coincide with those of the simulation results, validating our analysis. Next, from Fig. 4, we can see the trade-off between the retrieval accuracy and \bar{E} through the value of ζ . Specifically, the higher ζ leads to small \bar{E} because of the shorter memory activation time, but the IoT device might fail to serve the query, deteriorating the retrieval accuracy. Next, from Fig. 4, for the range of smaller ζ (e.g., $\zeta=0$), we can see that the retrieval accuracy becomes smaller as λ becomes smaller.

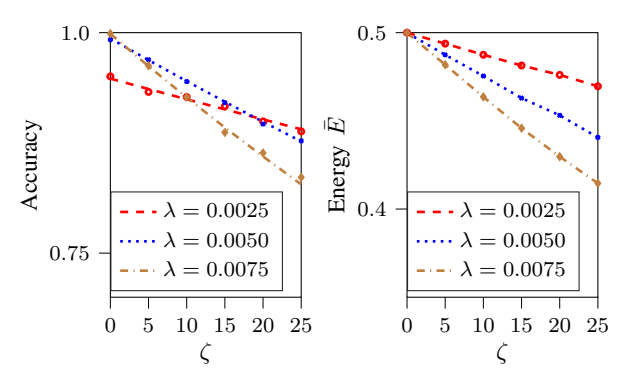


Fig. 4: Retrieval accuracy and normalized energy consumption obtained by analysis (line) and simulations (marker) against ζ .

When the ES activates the memory earlier time, the model in the memory gradually degrade as per refreshment until the end of the episode. As the memory activation time $(t_q - \zeta - T_{\Sigma})$ becomes larger as λ becomes smaller, the retrieval accuracy for $\lambda=0.0025$ becomes smaller than that for $\lambda = 0.0075$. On the other hand, for the range of larger ζ , we can see that the retrieval accuracy for the $\lambda = 0.0075$ becomes smaller than that for $\lambda = 0.0025$. This is because when the ES decides to activate memory later time, there is a risk of query arrival at the ES before memory activation, especially when the value of λ is higher. In this case, the ES cannot serve the current tasks under the latency constraint, degrading the retrieve accuracy. On the other hand, from Fig. 4, we can see that E becomes small as λ increases due to the decreasing memory activation time. This result shows the importance of memory activation timing ζ considering the trade-off between total energy consumption and retrieval accuracy.

3) Impact of τ : Fig. 5 shows the set of normalized energy consumption and retrieval accuracy when we change the value of τ from [64, 320] ms with the interval of 32 ms, where we apply $\lambda = 0.0025$, $\zeta = 20$, N = 64, $\Delta = 0.1$, $T_{\Sigma}=0$, $w_{\rm c}=0$, and $w_{\rm l}=0$. From Fig. 5, we can see the trade-off between retrieval accuracy and normalized energy consumption, through the value of τ . For the smaller (larger) range of accuracy, each node applies relatively large (small) refresh period τ , which decreases (increases) the energy consumed by the refreshment, but the quality of retained data at the memory becomes small. Next, from Fig. 5, we can see that, as β becomes smaller, more energy is needed to reach the same level of retrieval accuracy. As the small β corresponds to the fast degradation of stored data in the memory. This requires for IoT device to apply smaller τ to realize the target accuracy level, which increases the total energy consumption due to the increasing number of refreshments.

B. Energy efficiency

To investigate the system level performance of our proposed scheme, we consider the six parameters settings for $(T_{\Sigma}, w_{\rm c}, w_{\rm l}, \beta)$ listed in Table I. These represent a wide range of values that allow us to compare our proposed scheme with

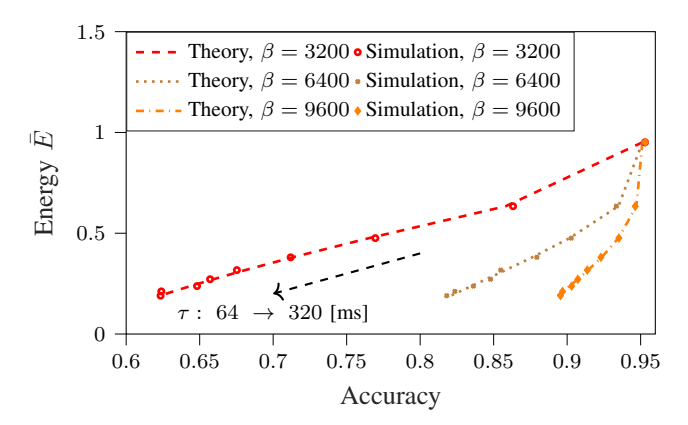


Fig. 5: The set of retrieval accuracy and normalized energy consumption for the different value of β where we vary the value of τ .

TABLE I: Parameter settings for the evaluation of energy efficiency.

Parameter	Setting					
	1	2	3	4	5	6
T_{Σ}	0	0	0	100	0	0
$w_{ m c}$	0	0	0	0	500	10^{5}
$w_{ m l}$	0	0	500	500	500	500
β	3200	6400	3200	6400	3200	3200

the baseline in terms of retrieval accuracy and normalized energy consumption under diverse conditions.

Fig. 6 shows the minimum \bar{E} against the retrieval accuracy constraint $U_{\rm th}$ with different settings, where we set $\lambda = 0.0025$, N = 64, and $\Delta = 0.1$. First, from Fig. 6, it can be observed that setting 3 always requires higher energy than setting 1. This is because of the additional energy required for model loading from the storage to the memory. Next, compared with settings 1 and 2, we can see that the minimum energy consumption of setting 2 is significantly smaller than that of setting 1, especially when $U_{\rm th}$ is small. In setting 2, as the accuracy degradation due to the lower refresh period becomes smaller for the larger β , the IoT device can assign the large τ to reach the retrieval accuracy requirement $U_{\rm th}$, reducing energy consumed by refreshments. Next, from Fig. 6, we can also see that the normalized energy consumption of setting 4 is smaller than that of settings 1 and 3 for the smaller range of $U_{\rm th}$ because of the larger β mentioned above. We can also see that the normalized energy consumption of setting 4 becomes highest when $U_{\rm th}=0.75$. This is because, in order to maintain the high retrieval accuracy, the ES requires to assign relatively small τ for memory refreshment, increasing the energy consumption at the memory in addition to the additional energy cost E_1 . Here, in setting 4, there are no values plotted for the range of $U_{\rm th} > 0.75$. This is because our proposed scheme can not provide retrieval accuracy higher than $U_{\rm th}$ due to the large overhead, T_{Σ} . Next, compared with the results of settings 3 and 5, we can see that \bar{E} increases as w_c increases. However, we can see that, even for the extreme case (setting 6), our proposed scheme can still offer smaller energy consumption than baseline scheme, i.e., E < 1, thanks

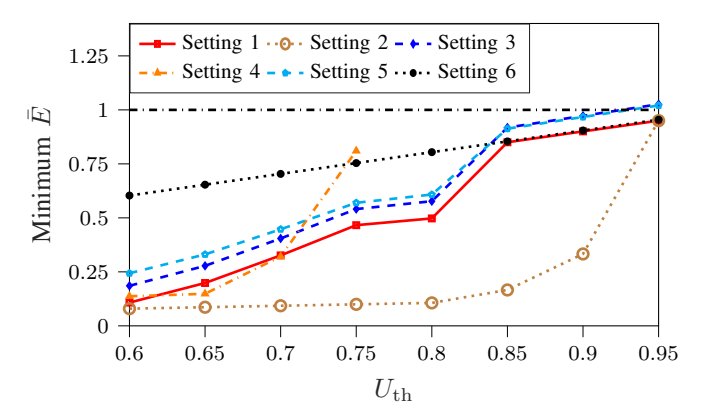


Fig. 6: Maximum Energy consumption against $U_{\rm th}$.

to the reduction of energy consumption required by DRAM refreshment by activating memory at the right time. Finally, we can see that in all settings, normalized energy consumption becomes larger as $U_{\rm th}$ becomes larger, while offering smaller energy consumption than always-on approach. The maximum retrieval accuracy constraint $U_{\rm th}$ under which our proposed scheme can achieve lower energy consumption than always-on approach are 0.95, 0.95, 0.9, 0.75, 0.9, and 0.95 for setting 1, 2, 3, 4, 5, and 6, respectively, indicating the efficiency of our proposed scheme.

V. CONCLUSION

We have proposed wireless memory activation and memory approximation for pull-based communication system, in which the ES remotely activates/approximates the DRAM memory for relevant ML model at the right timing. We analyzed the total energy consumption of the IoT device and retrieval accuracy of the proposed scheme considering the energy consumed by memory refreshment. The numerical results showed that our proposed scheme can realize high energy efficiency under the retrieval accuracy constraint, compared with the always-on approach. Future work includes the design of remote memory activation protocol for more general case considering the multiple tasks with different requirements.

APPENDIX-PROOF OF Eq. (7)

The Eq. (7) can be calculated as follows:

$$\Pr(N_{e}(M_{\zeta}) = k) = \sum_{m=0}^{\infty} \int_{m\tau+\zeta+T_{\Sigma}}^{(m+1)\tau+\zeta+T_{\Sigma}} {N \choose k} [1 - q_{e}^{m}]^{k} q_{e}^{m(N-k)} \lambda e^{-\lambda t} dt$$

$$\stackrel{(a)}{=} e^{-\lambda (\zeta+T_{\Sigma})} \sum_{m=0}^{\infty} \psi^{m} (1 - \psi) {N \choose k} [1 - q_{e}^{m}]^{k} q_{e}^{m(N-k)}$$

$$\stackrel{(b)}{=} e^{-\lambda (\zeta+T_{\Sigma})} (1 - \psi) {N \choose k} \sum_{j=0}^{k} {k \choose j} (-1)^{j} \sum_{m=0}^{\infty} \psi^{m} q_{e}^{mc}$$

$$\stackrel{(c)}{=} e^{-\lambda (\zeta+T_{\Sigma})} (1 - \psi) {N \choose k} \sum_{j=0}^{k} {k \choose j} (-1)^{j} \frac{1}{1 - \psi q_{e}^{c}}$$

where (a) $q_e=1-P_e$ and $\int_{m\tau+\zeta+T_\Sigma}^{(m+1)\tau+\zeta+T_\Sigma}\lambda\,e^{-\lambda\,t}dt=e^{-\lambda\,(\zeta+T_\Sigma)}\psi^m(1-\psi),$ with $\psi=\exp(-\lambda\,\tau);$ (b), we apply the binomial theorem $[1-q_e^m]^k=\sum_{j=0}^k\binom{k}{j}(-1)^jq_e^{mj};$ and (c) we put c=N-k+j and use $\sum_{m=0}^\infty\psi^mq_e^{mc}=\frac{1}{1-\psi\,q_e^c}$ where $0\leq\psi\,q_e^{N-k+j}\leq1.$

APPENDIX-PROOF OF EQ. (8)

The Eq. (8) can be calculated as follows:

$$\mathbb{E}[E_{\text{tot}}^{P}]$$

$$= \left(\int_{t=\zeta+T_{\Sigma}}^{\infty} \left(\lfloor \frac{t-\zeta-T_{\Sigma}}{\tau} \rfloor + w_{c} + w_{l} \right) \lambda e^{-\lambda t} dt \right) I_{M} \xi_{\text{re}}$$

$$= \left(\sum_{m=0}^{\infty} \int_{m\tau+\zeta+T_{\Sigma}}^{(m+1)\tau+\zeta+T_{\Sigma}} m \lambda e^{-\lambda t} dt \right)$$

$$+ \int_{t=\zeta+T_{\Sigma}}^{\infty} (w_{c} + w_{l}) \lambda e^{-\lambda t} dt \right) I_{M} \xi_{\text{re}}$$

$$= e^{-\lambda (\zeta+T_{\Sigma})} \left((1-\psi) \sum_{m=0}^{\infty} m \psi^{m} + (w_{c} + w_{l}) \right) I_{M} \xi_{\text{re}}$$

REFERENCES

- [1] X. Chen *et al.*, "Toward 6G native-AI network: Foundation model-based cloud-edge-end collaboration framework," *IEEE Commun. Mag.*, vol. 63, no. 8, pp. 23–30, 2025.
- [2] J. Shiraishi, M. Thorsager, S. R. Pandey, and P. Popovski, "TinyAirNet: TinyML model transmission for energy-efficient image retrieval from IoT devices," *IEEE Commn. Lett.*, vol. 28, no. 9, pp. 2101–2105, 2024.
- [3] S. Liu, K. Pattabiraman, T. Moscibroda, and B. G. Zorn, "Flikker: Saving dram refresh-power through critical data partitioning," in *Proc.* sixteenth Int. Conf. Architectural support Program. Lang. operating Syst., 2011, pp. 213–224.
- [4] I. Bhati, M.-T. Chang, Z. Chishti, S.-L. Lu, and B. Jacob, "DRAM refresh mechanisms, penalties, and trade-offs," *IEEE Trans. Comput.*, vol. 65, no. 1, pp. 108–121, 2015.
- [5] D. T. Nguyen, N. H. Hung, H. Kim, and H.-J. Lee, "An approximate memory architecture for energy saving in deep learning applications," *IEEE Trans. Circuits Syst. I: Regular Papers*, vol. 67, no. 5, pp. 1588– 1601, 2020.
- [6] R. Piyare, A. L. Murphy, C. Kiraly, P. Tosato, and D. Brunelli, "Ultra low power wake-up radios: A hardware and networking survey," *IEEE Commun. Surv. & Tut.*, vol. 19, no. 4, pp. 2117–2157, 2017.
- [7] V. Leon et al., "Approximate computing survey, part ii: Application-specific & architectural approximation techniques and applications," ACM Comput. Surv., vol. 57, no. 7, pp. 1–36, 2025.
- [8] S. Wang, M. N. Bojnordi, X. Guo, and E. Ipek, "Content aware refresh: Exploiting the asymmetry of dram retention errors to reduce the refresh frequency of less vulnerable data," *IEEE Trans. Comput.*, vol. 68, no. 3, pp. 362–374, 2018.
- [9] S. K. Ghosh, A. Raha, and V. Raghunathan, "Energy-efficient approximate edge inference systems," ACM Trans. Embedded Comput. Syst., vol. 22, no. 4, pp. 1–50, 2023.
- [10] E. C. Strinati et al., "Goal-oriented and semantic communication in 6G ai-native networks: The 6G-GOALS approach," in 2024 Joint Eur. Conf. Netw. Commun. & 6G Summit (EuCNC/6G Summit). IEEE, 2024, pp. 1–6.
- [11] A. Raha, S. Sutar, H. Jayakumar, and V. Raghunathan, "Quality configurable approximate dram," *IEEE Trans. Comput.*, vol. 66, no. 7, pp. 1172–1187, 2016.